3-2013

Deactivation mechanistic studies of copper chromite catalyst for selective hydrogenation of 2-furfuraldehyde

Dongxia Liu
Argonne National Laboratory

Dmitry Zemlyanov
Birck Nanotechnology Center, Purdue University, dimazemlyanov@purdue.edu

Tianpin Win
Argonne National Laboratory

Rodrigo J. Lobo-Lapidus
Argonne National Laboratory

James A. Dumesic
University of Wisconsin - Madison

See next page for additional authors

Liu, Dongxia; Zemlyanov, Dmitry; Win, Tianpin; Lobo-Lapidus, Rodrigo J.; Dumesic, James A.; Miller, Jeffrey T.; and Marshall, Christopher L., "Deactivation mechanistic studies of copper chromite catalyst for selective hydrogenation of 2-furfuraldehyde" (2013). *Birck and NCN Publications.* Paper 1356.
http://dx.doi.org/10.1016/j.jcat.2012.10.026

Authors
Dongxia Liu, Dmitry Zemlyanov, Tianpin Win, Rodrigo J. Lobo-Lapidus, James A. Dumesic, Jeffrey T. Miller, and Christopher L. Marshall

Journal of Catalysis 299 (2013) 336–345

Contents lists available at SciVerse ScienceDirect

Journal of Catalysis

journal homepage: www.elsevier.com/locate/jcat

Deactivation mechanistic studies of copper chromite catalyst for selective hydrogenation of 2-furfuraldehyde

Dongxia Liu [a], Dmitry Zemlyanov [b], Tianpin Wu [a], Rodrigo J. Lobo-Lapidus [a], James A. Dumesic [c], Jeffrey T. Miller [a], Christopher L. Marshall [a,*]

[a] Chemical Science and Engineering Division, Argonne National Laboratory, Argonne, IL 60439, USA
[b] Birck Nanotechnology Center, Purdue University, W. Lafayette, IN 47907, USA
[c] Department of Chemical and Biological Engineering, University of Wisconsin, Madison, WI 53706, USA

ARTICLE INFO

Article history:
Received 1 August 2012
Revised 24 October 2012
Accepted 24 October 2012
Available online 4 December 2012

Keywords:
Selective hydrogenation
2-Furfuraldehyde
Furfural alcohol
Deactivation
Copper chromite
X-ray Absorption Fine Structure (XAFS)
X-ray Photoelectron Spectroscopy (XPS)
Biofuel

ABSTRACT

Deactivation mechanisms of copper chromite ($CuCr_2O_4$·CuO) catalyst for vapor-phase selective hydrogenation for furfuryl alcohol have been investigated using *ex situ* and *in situ* X-ray absorption fine structure (XAFS), X-ray photon spectroscopy (XPS), and Auger Electron Spectroscopy (AES). At 200 °C, the catalyst steadily deactivated. One of the dominant origins of catalyst deactivation is poisoning due to strong adsorption of polymeric species formed from the reactant and/or products. Metallic Cu is identified as the active site, while loss of active Cu(I) sites due to hydrogenation is not a deactivation cause, as opposed to previous literature reported. The copper chromite catalyst showed low activity at 300 °C process temperature. Under this condition, the Cu particle size does not change, but Cr/Cu ratio increases by 50%, suggesting that Cr coverage of Cu sites becomes an additional cause of catalyst deactivation at this temperature, along with the poisoning deactivation mechanism at 200 °C.

1. Introduction

Fossil fuels provide the majority of our current energy supply. This is especially true in the transportation fuel sector, where about 94% of the transportation energy consumed in 2010 was derived from petroleum [1]. At the current rate of consumption, the currently known resources are estimated to last about 40 years [2]. Additionally, emission of greenhouse gases from petroleum combustion and security risk from imported oil are becoming more serious concerns. Accordingly, it is timely and desirable for the transportation energy system to shift from the current petroleum-based fuels to renewable sources. Biomass can be an ideal solution to the above problems due to its abundance and sustainability, being the only renewable source to supplement or even substitute for petroleum in the production of fuels. In 2009, biomass is the single-largest renewable energy resource, at 51% of total renewable energy consumption [3].

Unlike sugar/starch or lipids, lignocellulosic biomass will not impact food supplies for people. Hemicellulose is the second largest component at about 20–35% of total lignocellulosic biomass. The major components of hemicellulose are pantosans and xylans, which are C_5 polysaccharides. As shown in Fig. 1, 2-furfuraldehyde (furfural) can be derived from C_5 sugars by acid-catalyzed deconstruction of the long carbon chain to yield xylose, the monomer, followed by successive dehydration of the latter under the same acid environment [4]. Hydrogenation of furfural yields furfuryl alcohol and conversion of furfuryl alcohol to levulinic acid has been accomplished by acid hydrolysis in either water or organic solvents [5]. Levulinic acid is a versatile intermediate and can be converted to many other chemicals products. For example, using carbon supported Ru as catalyst, levulinic acid can be hydrogenated to water soluble γ-valerolactone (GVL), which is an important precursor for the production of hydrocarbon fuels [6]. Recently, Bond et al. have developed a dual-reactor process that can upgrade GVL to butene isomers and then oligomerized to C_{8+} alkanes, which are compatible with conventional fuels [7].

Selective hydrogenation of furfural to furfuryl alcohol is an important step along the route in the conversion of hemi-cellulosic materials to biofuels as listed in Fig. 1. High yield of furfuryl alcohol (>96%) has been achieved via liquid phase, batch hydrogenation using copper chromite ($CuCr_2O_4$·CuO) as the catalyst, with or without oxides of alkali–earth metals (CaO, BaO, or ZrO) as promoters. Typically, reactions are conducted under mild temperature (lower than 180 °C) and high hydrogen pressure (1000–1500 psi or even higher) [8–11]. However, the major problem of liquid-phase

* Corresponding author.
E-mail address: marshall@anl.gov (C.L. Marshall).

0021-9517/$ - see front matter © 2012 Elsevier Inc. All rights reserved.
http://dx.doi.org/10.1016/j.jcat.2012.10.026

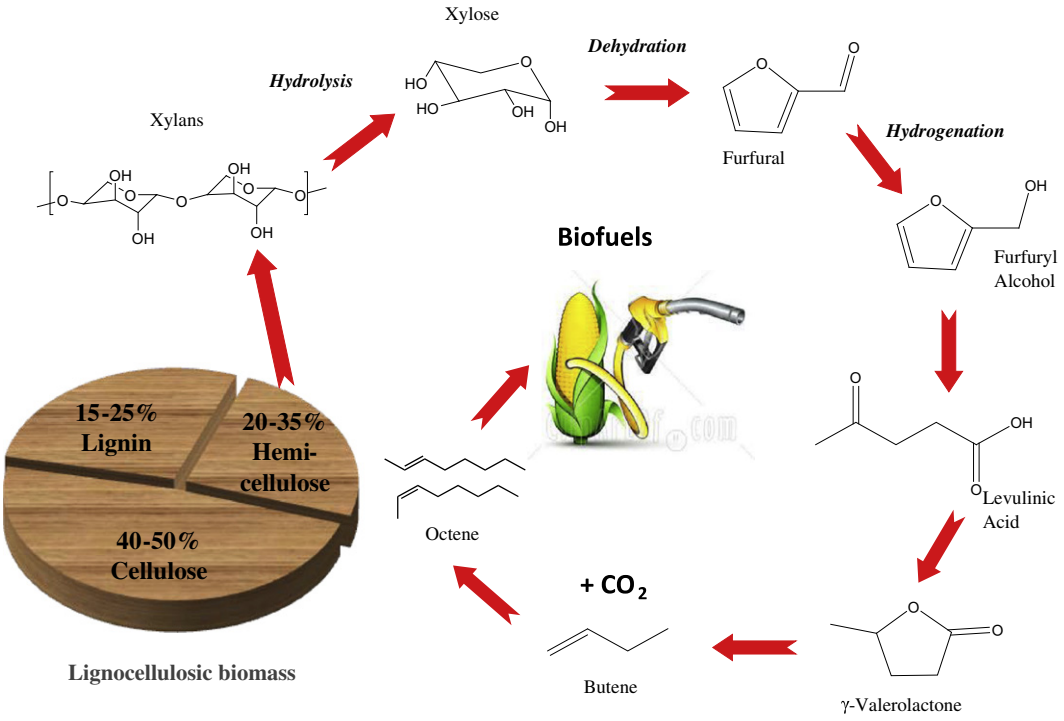

Fig. 1. Tentative route for conversion of hemi-cellulosic materials to biofuels.

process is that it is a batch and thus is not economically attractive for large-scale fuel applications. In addition, the catalyst is toxic due to the presence of Cr_2O_3, which can cause severe environmental pollution. Ni- or Co-based mono- or multi-metallic catalysts, such as Raney Ni [12,13], Ni—B [14,15], Ni—Co—B [16], Ni—Fe—B [17], Ni—Ce—B [18], Ni—P—B [19] and Ni—Mo—B [20], are non-toxic and therefore have been intensively investigated to substitute copper chromite for this purpose. However, these catalysts exhibit unsatisfactory performance especially the low selectivity to the desired product, thus preventing their further application for furfuryl alcohol production [17,19].

To obviate the high operating costs of using batch reactors and expensive equipment required for high pressure in the liquid-phase process, efforts have been made to convert furfural to furfuryl alcohol in vapor-phase continuous processes. Cu-based catalysts are exclusively used for this process [21–24] and in some cases promoted with either Cr [24,25] or alkali–earth metal oxides [26,27] to improve their performance. Other metal catalysts, such as Pt [28] or Pd [29–31], are rarely reported. However, two major difficulties have been encountered during vapor-phase hydrogenation of furfural. One difficulty is that hydrogenation products in all these cases contain considerable quantities of 2-methylfuran when high conversions of furfural are reached, making yield to the desired product uncompetitive to the commercial liquid-phase process [21,25]. Reaction pathway studies indicate that furfural is converted to furfuryl alcohol first, but subsequent dehydration and hydrogenation forms 2-methyl furan [21,26,30,32,33]. Catalyst deactivation is also a problem. Several possible deactivation mechanisms have been proposed, such as coke formation, change in the oxidation state of the copper, and sintering of Cu particles during the reaction process [34].

In this study, we examine deactivation mechanisms of copper chromite ($CuCr_2O_4{\cdot}CuO$) catalyst for selective hydrogenation of furfural to furfuryl alcohol in vapor phase. *In situ* X-ray Absorption Fine Structure (XAFS) was used to monitor the active copper oxidation states under reaction conditions. X-ray Photon Spectroscopy (XPS) was used to identify the surface composition as well as the oxidation state. Metallic Cu particle size after different pretreatment/reaction conditions was also examined by XAFS. A correlation of physical/chemical properties of copper chromite catalyst with their kinetic behavior for furfural hydrogenation under various conditions was established. This relationship leads to an understanding of the deactivation mechanisms of copper chromite catalyst for vapor-phase processes.

2. Materials and methods

2.1. Materials

The commercial copper chromite catalyst (Cu 1800P) was obtained from BASF. 2-Furfuraldehyde (Reagent, >99%) was purchased from Sigma–Aldrich and used as received. Hydrogen and nitrogen gases were all UHP level, obtained from Airgas.

2.2. Vapor-phase hydrogenation of 2-furfuraldehyde

Vapor-phase conversion of 2-furfuraldehyde (furfural) over copper chromite was conducted at atmospheric pressure in a ¼″ stainless steel tubular reactor placed in a clam-shell furnace equipped with temperature controllers. For each test, about 10–20 mg of copper chromite was diluted with SiC (100–140 mesh, mass ratio of sample to diluent is 1:9) to eliminate hot spots in the catalyst bed due to the exothermal nature of this reaction. The samples were then loaded onto a quartz wool bed, sitting on a 1/8″ stainless steel tubing located at the bottom half of the reactor to help fix the bed position.

Prior to reaction, the catalyst was reduced *in situ* in 10% H_2/N_2 for 1 h at 200 °C or 300 °C, respectively. After reduction, the furnace was set to the selected reaction temperature (between 150 °C and 300 °C) and the catalyst was kept under the same gas flow until the temperature was ready. Furfural was introduced to the reactor system by a carrier gas of H_2/N_2 sweeping through a bubbler containing pure furfural. This setup helped avoid furfural feed line

blockage problems when using a syringe pump. The temperature of bubbler remained constant via a circulating bath, and the furfural concentration reached steady state before starting the test by dialing the four-port valve (VICI Instruments) from bypass to reactor. Reactor effluents were analyzed by an online gas chromatography equipped with FID and packed column (EC-Wax, 30 m * 0.32 mm * 1 μm, ECONO-CAP, Grace Davison). All the chemical transfer lines and valves, from the bubbler to the online GC injector, as well as the gas sampling valve in the GC were heated to prevent condensation of either the reactant or the products.

Selective hydrogenation of furfural was studied isothermally at 150 °C, 200 °C, 250 °C and 300 °C, respectively. A typical reaction condition was 2% furfural and 50% H_2 to make the ratio of H_2: furfural = 25:1. One exception is for the test to determine selectivity at higher furfural conversion (>30%), where a lower furfural concentration (0.33%) was used, while the ratio of H_2 to furfural remained 25 for all the tests. Total gas flow rate was between 100 and 400 cc/min, where the furfural weight hourly space velocities (WHSV) were varied between 1 and 200 h^{-1}. WHSV was defined as the total mass flow rate of furfural divided by the total mass of copper chromite. Carbon balance was checked for each run and was in the range of 100 ± 5%. Since length to diameter (L/D) ratio of the diluted catalyst bed is larger than 3, the reactor can be assumed to operate under integral plug-flow conditions. Fresh catalyst was used each time to ensure that reactions were conducted under identical conditions.

2.3. X-ray Absorption Fine Structure (XAFS) data collection and analysis

X-ray adsorption measurements at Cu K-edge (8.9800 keV) were conducted on the bending magnetic beamline of the Material Collaborative Access Team (MRCAT, 10-BM) at the Advanced Photon Source (APS) at Argonne National Laboratory. Ionization chambers were optimized for the maximum current with linear response. A Cu foil spectrum was acquired simultaneously with each measurement for energy calibration. XAFS spectra were collected in transmission mode with minimum data point interval of 0.5 eV and each spectrum took about 15 min of scanning.

Copper chromite was diluted with silica gel (Davisil 644, Sigma–Aldrich) with mass ratio of 1:5. 6 mg of the above diluted sample was pressed into a cylindrical holder, with a thickness chosen to give a total absorption of approximately 2.0 ($\mu\chi$), which resulted in a copper edge step ($\Delta\mu\chi$) of ca 0.5. Proper amounts of CuO and Cu_2O standards (Sigma–Aldrich) were also loaded to collect spectra from reference compounds. The sample holder was placed into a continuous flow reactor, which was a quartz tube (1″ OD and 10″ length) sealed at both ends with Kapton windows and valves to isolate the reactor from the atmosphere. Copper chromite sample and the other two standards (CuO and Cu_2O) were scanned before any treatment and named "as is".

Copper chromite loaded in sample holders was reduced in 10%H_2/He (100 ml/min) at 200 °C and 300 °C for 1 h, respectively, purged with He for 15 min and cooled to room temperature in the flowing He. The temperature of the samples was controlled by thermocouples inserted into the reactor near the sample position. The two ball valves were closed after cooling to keep the samples in an inert environment, and XAFS spectra were collected on the reduced samples at room temperature. Traces of oxygen and moisture were removed from the gases by online traps before the gases contacted the samples. The above experiments are referred to as *ex situ* XAFS tests.

In situ XAFS measurements were performed under furfural hydrogenation reaction conditions. The same quartz tube reactor and sample holder were set up horizontally to allow X-ray transmitted through the sample wafer. A coaxially installed clam-shell furnace was used to heat the samples. Diluted copper chromite catalyst was reduced in 10%H_2/He (100 ml/min) at 200 °C for 1 h. The sample at this point in the experiment is referred to as fresh catalyst. About 0.33% of furfural was then flowed into the reactor by passing 10%H_2/He through a bubbler containing pure furfural. A four-port two-position actuator (VICI instrument) was used to switch the gas flow to ensure that the fresh catalysts remained in the reduced state without expose to air residual in the tubing. The hydrogenation reaction remained at 200 °C for 4 h before shut down. XAFS spectra were collected continuously throughout both the reduction and reaction processes every 15 min.

XAFS raw data were energy calibrated and normalized using WINXAS 3.1 software. The absorptive edge energy (E0) was determined from the initial maximum in the first-derivative spectrum. Phase shift, backscattering amplitude functions, and XANES reference spectra were determined experimentally from the Cu foil for Cu—Cu (12 at 2.556 Å) and reference compounds of Cu_2O and CuO. A standard procedure was employed to extract EXAFS parameters from sample spectra to obtain coordination number, bond distance, and Debye–Waller factor using least square fits in q- and r-space of the isolated, k^2-weighted Fourier Transform data. Finally, Cu particle size was estimated from Cu—Cu coordination number (N) using a modified empirical correlation developed by Miller et al. [35].

2.4. X-ray Photoelectron Spectroscopy (XPS) and X-ray Excited Auger Electron Spectroscopy (XEAES)

XPS and XEAES studies were performed using a Kratos Axis Ultra DLD spectrometer at the Birch Nanotechnology Center at Purdue University. Al Kα radiation (1486.6 eV) was used, and the X-ray gun operated at 75 W. The survey and high-resolution spectra were collected at a pass energy of 160 and 20 eV, respectively. The Kratos charge neutralizer was used for charge compensation of non-conducting samples.

The spectrometer is equipped with a catalytic cell (CatCell), in which a sample can be treated at elevated temperatures up to 1000 °C and 7 bar in either oxidative or reductive environment, and the sample can then be transferred to the analysis chamber without exposure to air within a few minutes. XPS spectra were acquired from copper chromite samples without any treatment and then after reduction in the CatCell in 5% H_2 for 1 h at 200C° and 300 °C, respectively. XPS analysis was also performed on reference compounds of Cu_2O and CuO. Used catalysts were investigated after remaining online for 4 h under various conditions without any further treatment in the CatCell of the XPS spectrometer.

CasaXPS 2.3.1dev85 was used to analyze XPS spectra. The C 1s peak at 284.80 eV from adventitious carbon was used as an internal standard for the charge correction. The elemental composition was calculated after Shirley or linear background subtraction using Scoefield Relative sensitivity factors accounting for different information depth. The C 1s and Cr 2p regions were curve-fitted using a Gaussian–Lorenzian function, whereas the Cu 2p and Cu LMM regions were fitted using the peaks obtained from the reference compounds (Cu, Cu_2O and CuO).

3. Results

3.1. Vapor-phase hydrogenation of 2-furfuraldehyde

Before evaluating the catalysts, a blank experiment was performed on SiC to determine its influence on reaction activity. The concentration of furfural remained constant during the test, indicating that no reaction occurred on the diluent. To minimize internal mass transfer limitation, copper chromite samples were

successively ground to fine powder before use. To examine external mass transfer limitation, a control experiment was conducted as following: the bubbler containing pure furfural was set at 62.5 °C, which gives 0.365 psi of furfural partial pressure or ~2% furfural at 1 atmospheric pressure. The reactor was loaded with 10 mg of copper chromite mixed with 90 mg of SiC, and three total gas flow rates of 100, 200, and 400 cc/min were swept through the bubbler, giving a WHSV of furfural 52, 103, and 206 h^{-1}. The reaction rates at 4-h-online have a linear relationship with the reciprocal of furfural space velocity, while furfural conversions were kept less than 20%. This linear correlation indicates that there was no external mass transfer limitation under the above reaction conditions. As a result, 10 mg of copper chromite mixed with 90 mg of SiC and 100 cc/min total gas flow (corresponding to 52 h^{-1} furfural WHSV) were selected as standard conditions.

Reaction kinetics data were collected under various conditions during vapor-phase hydrogenation of furfural. As an example, Fig. 2 shows profiles of furfural reaction rate, furfural conversion, and selectivity as a function of time on stream under standard conditions. The catalyst was reduced *in situ* in 10% H_2 for 1 h at 200 °C, and the reaction was operated at the same temperature. Carbon balance remained constant throughout the reaction process at about 98 ± 5%, which indicates that all the reaction products were detected. Two products were detected from the reactor effluent, which were furfuryl alcohol, the desired product and 2-methyl furan, a by-product. This result is consistent with other literature reports [21,25], indicating that dehydration of furfuryl alcohol forms 2-methyl furan [21,26,30,32,33]. Severe catalyst deactivation was observed, also in agreement with previous reports [21,24,25,34]. Furfural conversion dropped from initial 22% to 10% within 4 h. The instantaneous reaction rates (displayed at right y axis) decreased from 24 to 12 μmoles/s/g cat. This reaction was continuously run for another 20 h (data were truncated) under identical conditions to investigate the long-term deactivation phenomena. Stable conversion was not observed throughout the test, and the reaction rate decreased monotonically throughout the test.

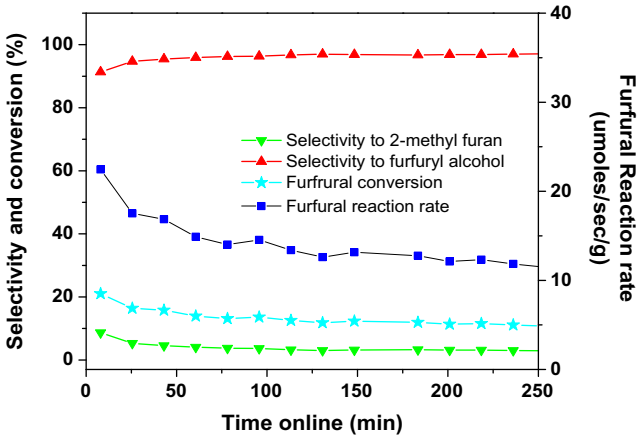

Fig. 2. Selective hydrogenation of furfural over copper chromite.

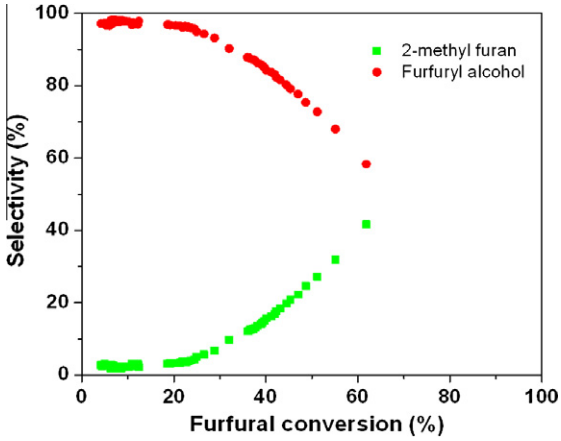

Fig. 3. Selectivity to furfuryl alcohol and 2-methyl furan as a function of furfural conversion.

To examine selectivity at higher furfural conversion, several sets of experiments were conducted using a high catalyst loading (20 mg) and lower furfural space velocities (4.2 h^{-1}). Selectivity to furfuryl alcohol and 2-methyl furan as a function of furfural conversion is plotted in Fig. 3. These experiments show that 2-methyl furan is the secondary product from conversion of furfuryl alcohol, as the selectivity of the former approaches zero when the conversion goes to zero. Therefore, on copper chromite catalyst, the reaction pathway can be described as follow:

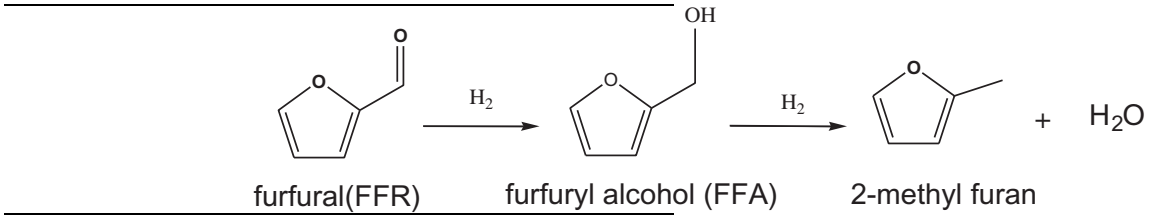

From Fig. 3, it can be seen that as the conversion increases, selectivity to furfuryl alcohol (red[1] line) decreases, lowering the yield. This behavior is one of the problems that make the vapor-phase process unfavorable, since it is difficult to stop the reaction at furfuryl alcohol.

Catalyst deactivation is the other problem that limits the application of copper chromite vapor-phase processes. To elucidate the deactivation mechanism, the effects of temperature on reaction rates were investigated by conducting a series of control experiments under various pretreatment and reaction temperatures under standard catalyst loading and furfural WHSV (52 h^{-1}). Copper chromite deactivated in all of these control experiments, and stable performance was not obtained during the 5–6 h reaction test. For comparison, the reaction rate at the time point of 4-h-online was chosen.

Fig. 4 represents the reaction rate of furfural after 4-h-online. At a reaction temperature of 200 °C, the effect of reduction temperature (none, 200 °C and 300 °C) on reaction rates was determined. Reduction of copper chromite at 200 °C for 1 h gave the most active catalyst, with furfural reaction rate of 22 μmoles/s/g cat. After reduction at 300 °C, the reaction rate of 6 μmoles/s/g cat was only

[1] For interpretation of color in Figs. 3 and 5–8, the reader is referred to the web version of this article.

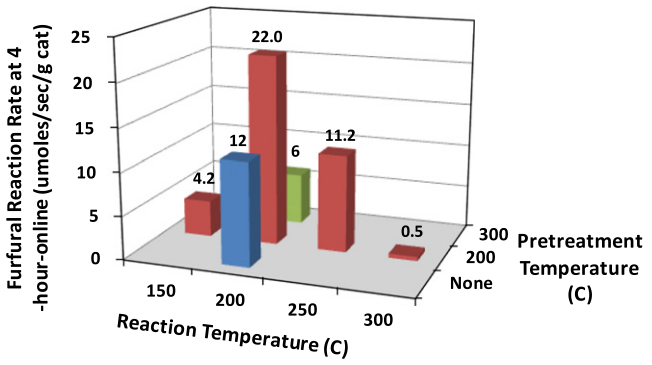

Fig. 4. Furfural reaction rates at 4-h-online under various pretreatment temperatures and reaction temperatures.

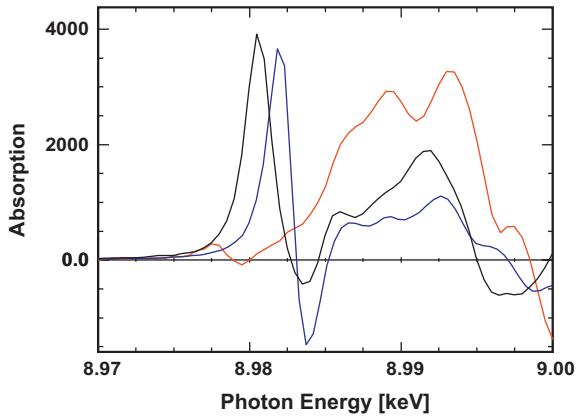

Fig. 5b. First derivatives of XANES spectra of references of copper chromite ($CuCr_2O_4$·CuO) (red), cuprous oxide (Cu_2O) (blue), and Cu foil (black) at Cu K-edge from 8.98 to 9.00 keV.

about 0.25 times of that after reduction at 200 °C. In contrast, the catalyst showed intermediate activity (12 μmoles/s/g cat) without pre-reduction. Since 200 °C was the optimum catalyst pretreatment temperature, it was selected for the following activity tests at different reaction temperatures.

After pretreated at 200 °C for 1 h, the furfural hydrogenation reaction was measured at 150 °C, 200 °C, 250 °C and 300 °C, respectively. The reaction rate profile has a volcano shape versus temperature, with the highest rate (22 μmoles/s/g cat) at 200 °C. There was very little conversion (0.5 μmoles/s/g cat) at 300 °C. Rates at 150 °C and 250 °C were only 0.5 and 0.5 times of the rate at 200 °C, respectively. When temperature reaches 300 °C, the reaction was low, with furfural conversion 0.5 μmoles/s/g cat.

3.2. X-ray Absorption Fine Structure (XAFS)

3.2.1. Ex situ experiment

XAFS measurements at Cu K-edge (8.9800 keV) were conducted on three reference compounds of copper chromite ($CuCr_2O_4$·CuO) (red), cuprous oxide (Cu_2O) (blue) and Cu foil (black), and the XANES are shown in Fig. 5a. The spectrum of non-reduced copper chromite (red) is shifted to higher energy, consistent with Cu^{2+} ions, for example, $Cu(NO_3)_2$. Cuprous oxide (Cu_2O) (blue) shows a big pre-edge feature and is shifted to lower energy. The edge energy of Cu foil (black) is shifted to even lower energy around 8.99–9.01 keV. The 1st derivative curves of the three reference spectra are shown in Fig. 5b, and the energy edge positions, determined from the initial maximum in the three curves, are 8.9800, 8.9814, and 8.9863 keV for Cu^0, Cu^{1+}, and Cu^{2+}, respectively. A reduction in the total electron density (from Cu^0 to Cu^{1+} and Cu^{2+}) results in an increase in the electron affinity, shifting the adsorption edge to slightly higher energy. This small shift in edge position is usually used to assign the different oxidation states.

The copper chromite catalyst was reduced in 10% H_2 at 200 °C and 300 °C, respectively, and the XAFS spectra were collected at room temperature. XANES spectra of copper chromite after reduction at 200 °C (red) and 300 °C (blue) are shown in Fig. 6a with Cu foil (black) for comparison. The position of the edge and intensity of the peak at about 8.995 keV from the three spectra completely overlap, which indicates that the copper chromite is fully reduced to the metallic state at 200 °C and 300 °C. The small changes in the shape of the two copper chromite curves from Cu foil between 8.985 and 8.990 keV are consistent with a minor amount of a second (metallic) scatter possibly from neighboring Cr atoms.

The first shell of EXAFS spectra were obtained by a Fourier transform (FT) of the k^2-weighted data from 2.7 to 10.8 $Å^{-1}$, and these results are shown in Fig. 6b with magnitudes in solid line and imaginary part in dashed line. Copper chromite after reduction at 200 °C is represented in the red line and 300 °C in the blue line. The two spectra lie on top of each other with no significant differences. EXAFS parameters, such as coordination number of Cu—Cu shell (N_{Cu-Cu}), bond distance (R), Debye–Waller factor (DWF) and edge energy shift (E_0), were extracted by fitting the above spectra, and these results are summarized in Table 1. Assuming hemispherical particle shape, the average Cu particle sizes were estimated [35], and these values are also given in Table 1. The last column

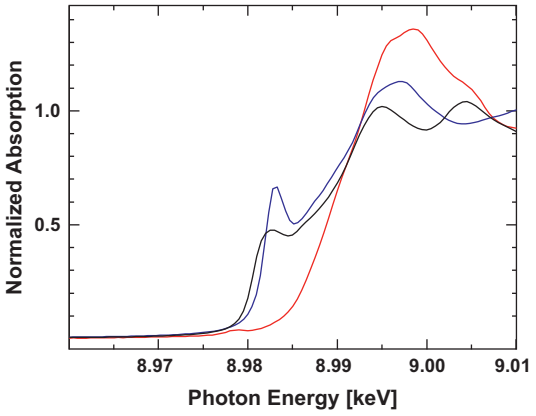

Fig. 5a. XANES spectra of references of copper chromite ($CuCr_2O_4$·CuO) (red), cuprous oxide (Cu_2O) (blue), and Cu foil (black) at Cu K-edge from 8.98 to 9.01 keV.

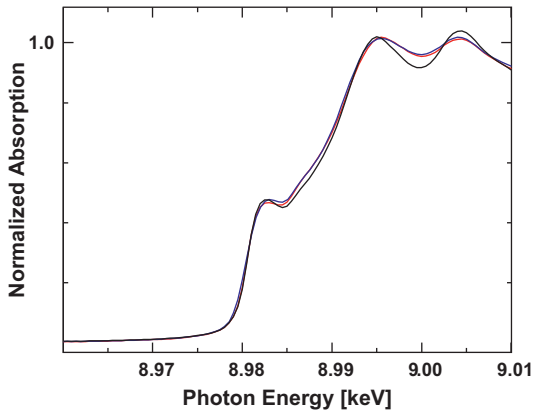

Fig. 6a. XANES spectra of copper chromite after *ex situ* reduction at 200 °C (red) and 300 °C (blue) and Cu foil (black).

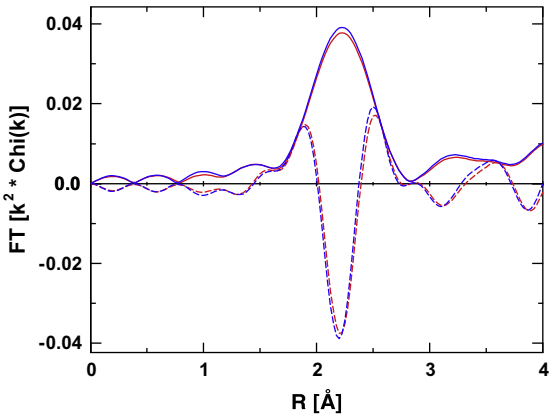

Fig. 6b. *Ex situ* EXAFS study of copper chromite after reduction at 200 °C (red) and 300 °C (blue), respectively. The solid line is the magnitudes and dashed line is imaginary part after Fourier Transform of the k^2-weighted data from 2.7 to 10.8 Å.

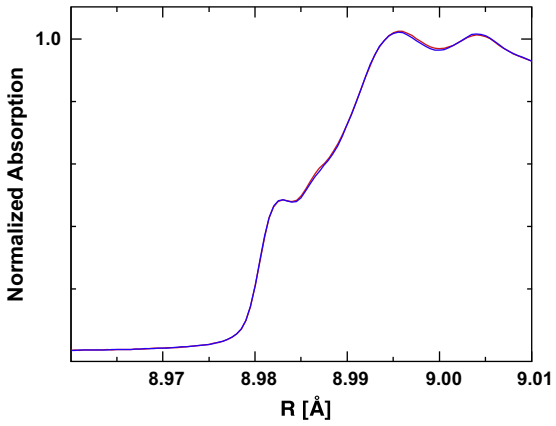

Fig. 7a. *In situ* XANES study of fresh and used copper chromite catalysts. Fresh catalyst is the red line, used catalyst is blue line, and black curve is Cu foil as reference.

of the table is Cu oxidation states, obtained from XANES spectra analysis from Fig. 6a. The results of fitting the copper chromite spectra after *ex situ* reduction at 200 °C and 300 °C are identical, showing a Cu—Cu contribution with a coordination number of 10 at an interatomic distance of 2.55 Å. The estimated Cu particle sizes after both pretreatments are the same within experimental error, which is around 5.0–5.5 nm. This result indicates that reduction at elevated temperature (300 °C) does not increase the Cu particle size significantly, nor do the Cu particles sinter at 300 °C, as compared to low-temperature reduction (200 °C). Additionally, there is no evidence of the existence of the second metal (Cr) in EXAFS analysis due to the fact that the bond distance ($R = 2.55$) is equal to the sum of the atomic radii of two Cu atoms, which is 2.556 Å. However, Cr has the same atomic radius and a similar number of electrons. Thus, it would not be able to detect in the EXAFS analysis even if they exist.

3.2.2. In situ experiment

Characterization of *ex situ* reduced samples indicates that Cu is fully reduced at 200 °C, and higher reduction temperature (300 °C) does not change the particle size. However, catalyst structures/properties may considerably differ under reaction conditions. Thus, *in situ* XAFS studies were carried out to explore the structure and property of copper chromite under furfural hydrogenation conditions.

Fresh copper chromite catalyst after *in situ* reduction at 200 °C for 1 h was studied at the same temperature. After 4 h of furfural hydrogenation at 200 °C, an XAFS spectrum was collected. XANES spectra of the fresh (red) and used (blue) catalysts at *in situ* experiment are shown in Fig. 7a. The spectrum of the used catalyst is identical to that of fresh catalyst, and both of them overlap with the Cu foil (not shown) edge position and the intensity of the peak at 8.995 keV. This result indicates that metallic Cu is present in the fresh catalyst, and Cu remains zero valent throughout the entire reaction process. Since no other oxidation state Cu species were identified, we can conclude that Cu^0 is the only active component for hydrogenation of furfural under the selected reaction conditions.

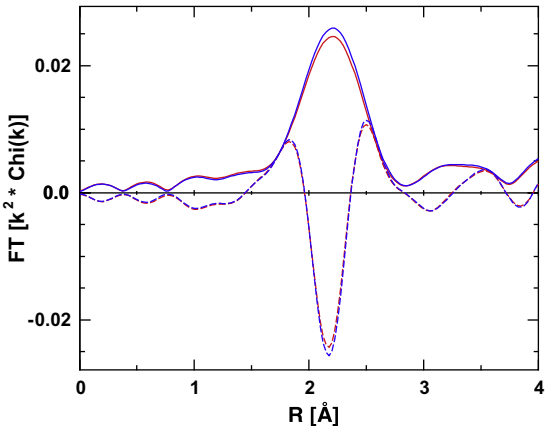

Fig. 7b. *In situ* EXAFS study of fresh (red) and used (blue) copper chromite catalysts.

Fig. 7b represents EXAFS spectra of fresh and used catalysts collected during the *in situ* experiment. The red line is for the fresh catalyst, and the used catalyst is shown in blue line. The solid curves are magnitudes, and the imaginary part after Fourier Transform is displayed in the dashed lines. There is no visible difference in the spectra of fresh and used catalysts, revealing that the reaction does not lead to any change in Cu nanoparticle size. The approximate Cu particle sizes from fitting EXAFS spectra are 5.5 nm for fresh catalyst and 6.5 nm for the used catalyst (as shown in the lower part of Table 1). Given the 10–20% experimental error of XAFS technique, we believe that the size of Cu nanoparticles do not sinter significantly after the reaction. The Cu—Cu bond distance *R* is not changed under reaction, which is 2.53 Å, close to the value

Table 1
EXAFS fit of copper chromite after *ex situ* reduction at 200 °C and 300 °C, as well as fresh and used catalysts at *in situ* experiments.

Experimental conditions	N_{Cu-Cu}	*R* (Å)	DWF ($\times 10^3$)	E_0 shift (eV)	Cu particle size (nm)	Cu oxidation state
Ex situ experiments						
Ex situ red. 200 °C	10.0	2.54	1.0	−0.6	5.5	Cu^0
Ex situ red. 300 °C	9.7	2.55	1.0	−0.6	5.0	Cu^0
In situ experiments						
Fresh catalyst	10.0	2.53	5.7	−1.9	5.5	Cu^0
Used catalyst	10.6	2.53	5.7	−1.7	6.5	Cu^0

of the Cu foil. Debye–Waller factor (DWF) is higher than at room temperature since the measurements were conducted at 200 °C.

3.3. X-ray Photoelectron Spectroscopy (XPS) and X-ray Excited Auger Electron Spectroscopy (XEAES)

Since XAFS provides information about bulk properties of a sample, XPS and XEAES were used to investigate surface properties of the samples. Table 2 shows the elemental composition (atomic %) calculated based on XPS data of copper chromite as received ($CuCr_2O_4$·CuO), after reduction in the CatCell for 1 h at 200 °C and 300 °C, respectively. The atomic ratio of Cr to Cu is reported in the same table. In general, reduction at elevated temperatures results in a noticeable increase in the Cr to Cu ratio in comparison with the as-received sample. This increase points to a change in the surface composition of catalyst due to reduction, which could be explained by either the decomposition of $CuCr_2O_4$ followed by Cr species covering Cu surface, or by agglomeration of Cu species into larger particles [36,37]. However, the second possibility can be ruled out based on the results obtained from *ex situ* XAFS, where we found that Cu particles remain the same size after reduction at 300 °C and significant sintering did not occur. In particular, the Cr to Cu area ratio increased up to 1.9 after reduction at 300 °C, which is almost 50% more than the value of 1.4 observed after reduction at 200 °C. Since Cr is not active for the reaction, it would be reasonable to deduce that samples having higher Cr to Cu ratios would have lower activity. This expectation is consistent with the results of catalyst activity test, where the sample after reduction at 300 °C shows a lower rate (6 μmoles/s/g cat), as compared to 22 μmoles/s/g cat for the sample after reduction at 200 °C.

Cu oxidation states were determined using XPS and XEAES and Fig. 8 shows the Cu $L_3M_{4,5}M_{4,5}$ Auger spectra of copper chromite as received ($CuCr_2O_4$·CuO) and after reduction at 200 °C (Red 200 °C) and 300 °C (Red 300 °C), respectively. It is challenging to separate the Cu(I) and Cu(0) components in the Cu 2p regions; therefore, the Cu LMM Auger lines were used to distinguish various Cu oxidation states [36–42]. In this study, the reference Auger spectra of CuO (red), Cu_2O (blue), and Cu^0 (green) were collected first, and their corresponding kinetic energy positions were reported in Table 3. Auger spectra from the samples were curve-fitted using the reference spectra as line shapes, and the surface compositions of the Cu species are presented in Table 3. A similar approach was used for curve fitting of the Cu 2p spectra, and the quantitative results were consistent with the Auger results. Cu(II) is the major component(~80%) of copper chromite ($CuCr_2O_4$·CuO) before any reduction, and the remainder is Cu(I) (~20%). The Cu(0) contribution is negligible. However, after reduction at 200° C and 300 °C, the Cu(0) species dominates, rendering the two Cu oxidized species insignificant. This result is consistent with the XAFS results, where

Table 2
XPS analysis of surface elemental composition of copper chromite catalyst before any pretreatment ($CuCr_2O_4$·CuO), after reduction at 200 °C and 300 °C, respectively.

Sample	Atomic composition (%)				Cr/Cu
	C 1s	Cr 2p	Cu 2p	O 1s	
$CuCr_2O_4$·CuO	7	16	22	55	0.7
Red 200 °C	21	18	13	48	1.4
Red 300 °C	10	25	13	52	1.9
Fresh catalyst	21	18	13	48	1.4
Used catalyst	28	13	11	48	1.2

Table 3
Various Cu oxidation species on copper chromite samples before any pretreatment ($CuCr_2O_4$·CuO), after reduction at 200 °C and 300 °C, respectively, obtained from Cu $L_3M_{4,5}M_{4,5}$ Auger spectra.

Species	Kinetic energy (eV)	Composition (%)		
		$CuCr_2O_4$·CuO	Red 200 °C	Red 300 °C
Cu(0)	918.3	2	94	95
Cu(I)	916.8	19	4	5
Cu(II)	917.8	79	2	0

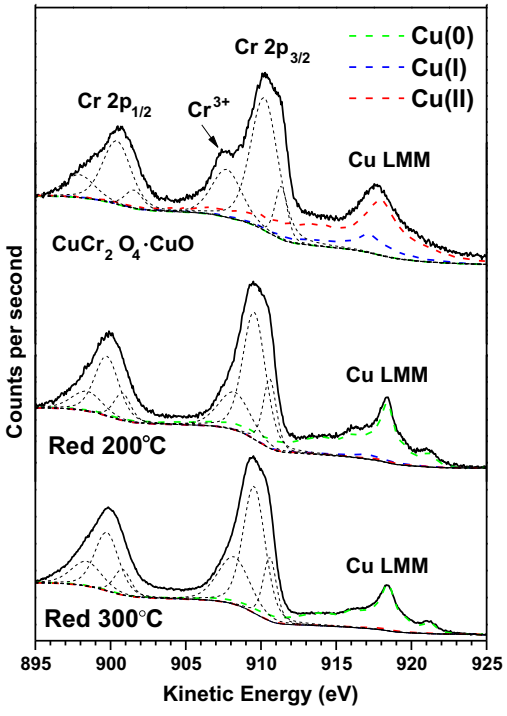

Fig. 8. Cu LMM Auger spectra of Cu, CuO, Cu_2O, and $CuCr_2O_4$·CuO.

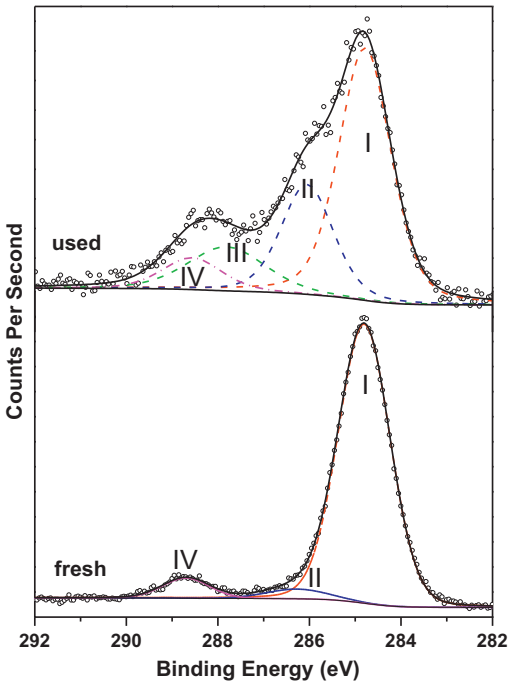

Fig. 9. Carbon 1s electron spectra from fresh catalyst (after *in situ* reduction at 200 °C) and used catalyst (stay online for 4 h).

Table 4
XPS analysis of various carbon oxide species on fresh and used catalysts.

	Species	Binding energy (eV)	Atomic composition (%)	
			Fresh catalyst	Used catalyst
Peak I	Adventitious (C—C)	284.8	90	55
Peak II	Alcohol or ether (C—OH or C—O—C)	286.1–286.3	4	24
Peak III	Carbonyl (C=O)	287.8	–	14
Peak IV	Carboxyl or ester (O—C=O)	288.6–288.7	6	7

copper chromite is fully reduced to the metallic state at 200 °C and 300 °C. In addition, one can also conclude that the samples have uniform surface and bulk compositions under above conditions.

Elemental compositions of "fresh" and "used" catalysts are shown in the bottom half of Table 2. The copper chromite sample after reduction at 200 °C is designated as "fresh" catalyst, while "used" catalyst is from the reactor after remaining online for 4 h under "standard conditions" after a pre-reduction temperature of 200 °C. There are more carbon atoms on the "used" catalyst surface than its fresh counterpart, which indicates the presence of reactant, product, or coke deposition on the used catalyst. To further explore these carbon species, each C 1s spectrum of fresh and used catalysts was curve-fitted with four individual components that represent adventitious carbon (C—C, peak I, 284.8 eV), carbon present in alcohol or ether groups (C—OH or C—O—C, peak II, 286.1–286.3 eV), carbonyl group (C=O, peak III, 287.8 eV) and carboxylic or ester groups (O—C=O, peak IV, 288.6–288.7 eV) [43–45], as shown in Fig. 9, and the corresponding compositions are reported in Table 4. Spectral contributions from peak II (alcohol or ether) and peak III (carbonyl species) in the used catalyst are significantly greater than those in the fresh catalyst, which can be explained by the deposition of both the reaction product (furfuryl alcohol, peak II) and reactant (furfural, peak III) on the copper chromite surface.

4. Discussion

4.1. Copper chromite deactivation mechanisms

Severe deactivation of the copper chromite catalyst used for vapor-phase hydrogenation of furfural has been reported by others [34]. Several possible mechanisms have been proposed, such as (a) loss of the active Cu(I) species by reduction, (b) Cu particle sintering, and (c) active Cu site coverage by coke or adsorbed reactants/products. Cu sites may also be covered due to metal migration in bimetallic or alloy catalysts cases.

The nature of the active species of copper chromite catalysts in methanol formation, methanol decomposition, and other reactions has been the center of debate for many years. It has been widely accepted that Cu(I) is involved in the active site and it is stable under reaction conditions existing as $CuCrO_2$ crystalline phase. Cr is not an active component for activity, but it stabilizes Cu(I) from being reduced [46–49]. There are some literature reports that metallic Cu functions as a promoter to Cu(I), and a synergic effect has been invoked for optimum activity [34,36,40,50]. Nishimura et al. have reported that 1,3-butadiene hydrogenation proceeds on metallic copper [51], Deutsch and Shanks also found that Cu(0) is primarily responsible for the activity of 5-methylfurfuryl alcohol hydrogenolysis since there is a linear correlation between specific activity and surface concentration of Cu(0) [37]. Stroup investigated copper chromite activity for low-temperature hydrogenation and found that the catalyst was partially or completely reduced to metallic copper [52]. Despite these many studies of copper chromite, disagreement still remains about the relationship between preparation procedure, activation protocol, and final active sites. Based on our results from *in situ* XAFS experiments, we conclude that copper chromite is fully reduced to the metallic state at 200 °C in H_2, and Cu remains zero valent under reaction conditions, as shown in Fig. 7a. No other Cu oxide species were detected from XAFS experiments. On the other hand, AES data confirmed the existence of Cu(0) species as the major surface component (94%) in the reduced sample (Red. 200 °C) in Table 3 and Fig. 8. Negligible amounts of Cu(I) and Cu(II) are possibly within the experimental error. Therefore, we believe that Cu(0) is the primary active component for furfural hydrogenation and loss of active Cu(I) species is not the cause of deactivation of copper chromite.

Sintering processes are thermally induced and typically have an exponential relationship with temperature. It is generally accelerated by the presence of water vapor. Usually, sintering occurs more readily on metals with lower melting points, such as Ag, Cu, and Ni [53]. For instance, Houel et al. reported that Cu sintering was one of the major causes of deactivation of Cu/ZSM-5 catalyst for HC-SCR under simulated diesel exhaust emission conditions [54]. Martínez-Arias et al. observed a deactivation process taking place rapidly on CuO/CeO catalysts for preferential CO oxidation in rich H_2 conditions and attributed this deactivation to copper sintering in the course of the run [55]. However, Cu sintering is not the cause of deactivation of copper chromite for furfural hydrogenation. According to XAFS data, the Cu particle sizes are similar before and after reaction, as shown in Table 1 *in situ* experiments section. Average Cu particle sizes are about 6 nm in fresh and used catalysts. The small difference is within the experimental error of the XAFS technique, which is usually around 10–20%. The reaction temperature was 200 °C, which was relatively low for Cu sintering.

At 200 °C, Cu sites are covered by coke formation and/or poisoned by species derived from adsorbed reactant product molecules, leading to deactivation based on the XPS analysis. Table 4 shows compositions of various carbon oxide species on "fresh" and "used" catalysts obtained from the C 1s region. "Fresh" catalyst was defined by copper chromite after reduction at 200 °C, and "used" catalyst designates pre-reduced copper chromite at 200 °C and also tested at 200 °C in the reactor. It is clear that there are more C—OH or C—O—C (peak II) and C=O (peak III) species on the used catalyst surface than the fresh catalyst. In particular, 24% of carbon on the used catalyst was contributed from C—OH or C—O—C species, which could be either furfuryl alcohol (C—OH group) or furfural (C—O—C) in our case. This amount is six times more than that on the fresh catalyst, which was only 6%. There are no carbonyl species (peak III) on the fresh catalyst, but these species account for 14% of carbon in the used catalyst, which could be explained by the adsorption of furfural. Contributions from carboxyl or ester groups (peak IV) are the same in the fresh (6%) and used (7%) catalysts, which indicates that carboxyl or ester species are not formed as side products during reaction process. This finding agrees with the catalyst evaluation result, where only furfuryl alcohol and 2-methyl furan were produced. Peak IV was also observed in CuO and Cu_2O Auger spectra at the same position with the peak area (not shown here) and therefore we believe it is

due to impurities. We note that migration of Cr onto Cu sites is not the reason for copper chromite deactivation at 200 °C conditions, since the Cr to Cu intensity ratios of the fresh catalyst and used catalyst are close, equal to 1.4 for fresh catalyst and 1.2 for used catalyst, as listed in Table 2. The small difference is within the experimental error.

After reduction at 300 °C for 1 h, the Cr to Cu ratio increases by 50% up to 1.9 as shown in Table 2 in sample "Red 300 °C", indicating that Cr covers about one half of the Cu surface sites. This behavior is likely to be the dominant reason for copper chromite deactivation at temperatures above 200 °C and explains the pretreatment temperature effect on activity in Fig. 4. Pre-reduction at 200 °C yielded the most active catalyst, with reaction rate of 22 μmole/s/g cat. However, the activity of copper chromite after pretreatment at 300 °C (6 μmole/s/g cat) was only about 0.25 times of that at 200 °C. Since reactions were conducted under exactly the same conditions, the difference in activity should only come from the effect of different pretreatment temperatures. Therefore, we believe that the Cr species from partial decomposition of copper chromite cover Cu active sites after pre-reduction at 300 °C and result in a lower activity. Our observation is consistent with the study of Limura et al. [36] who found that copper chromite samples after reduction at 200 °C and 400 °C have significantly higher Cr/Cu ratios than the fresh sample. The only difference between their work and the present study is that they used $CuCr_2O_4$, the spinel structure instead of $CuCr_2O_4$·CuO. Interestingly, the sample without any pretreatment shows moderate activity, equal to 12 μmole/s/g cat. This activity is because when the furfural and H_2 were flowing concurrently over the catalyst in the course of run, H_2 fully reduced the copper(II) species in copper chromite catalyst to metallic Cu at reaction temperature (200 °C), as proved by XAFS results. Furfural readily adsorbed on the "freshly" reduced Cu active sites and was then converted to furfuryl alcohol.

The effect of reaction temperature on catalyst activity after pretreatment at 200 °C in Fig. 4 has a volcano shape, with the highest rate at 200 °C. Reaction rates obtained above this temperature, such as 250 °C, are lower, and the reaction rate is very low at 300 °C. The reason for the low rate at higher temperatures is that both furfural and furfuryl alcohol are polymerized and adsorbed on the catalyst surface as carbonaceous deposits at elevated temperatures [22], and these species thus cover part of Cu active sites, which is the same origin of catalyst deactivation at 200 °C. Moreover, decomposition of copper chromite may also expose more Cr species to the catalyst surface. Therefore, we believe that combined coverage of Cu active sites by both the adsorption of chemicals and decomposed Cr species leads to deactivation of copper chromite when reactions were conducted at temperatures above 200 °C.

4.2. Implication for a biomass conversion process

Based on the previous discussion, we believe that when the reaction was conducted at 200 °C, coke formation and/or poisoning by species derived from adsorbed furfural and/or furfuryl alcohol is the most likely cause of deactivation of copper chromite for vapor-phase conversion of furfural to furfuryl alcohol. At temperatures above 200 °C, additional covering of Cu sites by Cr species from decomposed copper chromite materials adversely affects the catalyst activity significantly.

Sitthisa et al. [32] studied the adsorption patterns of furfural and furfuryl alcohol on Cu surface using DFT calculation. Their combined experimental and theoretical observations indicate that furfural interacts with the Cu surface via the lone pair of oxygen to produce η^1(O)-aldehyde species. Hydrogen atoms can attack either the C or O atom and convert them to the alkoxide or hydroxyalkyl intermediates, respectively, before furfuryl alcohol is produced. Therefore, a stable catalyst for vapor-phase conversion of furfural to furfuryl alcohol will require the surface of catalyst to be oxophobic, to weaken the adsorption of reactant and/or products, especially furfural alcohol. Theoretically, the optimum selections would be alkali or alkali earth metals or metals or metal oxides from group IIIb, IVb, and Vb due to their basic properties. It has been previously reported that Cu oxides promoted with Na_2SiO_3 [21,22,56] were good catalysts for vapor-phase conversion of furfural to furfuryl alcohol under atmospheric pressure. The yield of furfuryl alcohol can reach 99% over a wide temperature range between 260 °F and 300 °F (127 °C to 149 °C). Kozinski [56] and Bankmann et al. [23] used $CuCO_3$ promoted with Na_2SiO_3 on various silica supports as catalysts, and the productivity of furfuryl alcohol per pound of catalyst was significantly improved by employing high surface area silica materials. Alkali earth metal salts such as $Ca(NO_3)_2$ [8,57] and $Ba(NO_3)_2$ [8] were also used as promoters to Cu-based catalysts for the same purpose. Nagaraja et al. [26,58,59] developed a co-precipitation method to make a highly efficient Cu/MgO catalysts for the reaction. Both of the conversions of furfural and selectivity to furfuryl alcohol are above 98% at atmospheric pressure and 453 K.

Another way to improve catalyst stability and eliminate deactivation is to increase the hydrogen partial pressure and avoid elevated process temperatures. Recall that copper chromite has been proved to be a successful commercial catalyst for liquid-phase batch process for more than 5 decades when the conversion was performed under mild temperature (less than 180 °C) and high hydrogen pressure (more than 1000 psi) [8,9]. Mild process temperatures could diminish the Cr covering effect. In addition, higher hydrogen pressure could help to maintain a clean catalyst surface and prevent high coverages by species derived from adsorbed reactant and products. Therefore, a continuous process using mild temperature and high hydrogen pressure should be designed and test.

5. Conclusions

Copper chromite ($CuCr_2O_4$·CuO) was studied for vapor-phase hydrogenation of furfural under various pre-reduction temperatures and reaction temperatures. In addition to the poor selectivity at furfural conversions above 20%, severe catalyst deactivation was observed. *Ex situ* and *in situ* XAFS, XPS, and AES techniques were used to investigate deactivation mechanisms. Catalyst poisoning due to the adsorption of species derived from furfural and furfuryl alcohol are one of the dominant causes for deactivation when operated at 200 °C, as indicated by AES data of fresh and used catalysts. In contrast, loss of active Cu(I) sites due to hydrogenation can be ruled out based on *in situ* XAFS results, which show that metallic Cu is the active component for the reaction and copper is maintained in the metallic state throughout the process. Cu particle sintering is not a cause for deactivation due the relatively low reaction temperature, as proved by *in situ* XAFS experiments. However, when the process temperature is increased to 300 °C (either pre-reduction or reaction temperature), Cr species from partial decomposition of copper chromite cover active Cu sites, which becomes another phenomenon resulting in lower activity along with the poisoning effect by adsorbed species derived from furfural and furfuryl alcohol.

Acknowledgments

This material is based upon work supported as part of the Institute for Atom-efficient Chemical Transformations (IACT), an Energy Frontier Research Center funded by the U.S. Department of Energy, Office of Science, Office of Basic Energy Sciences. Use of the Advanced Photon Source is supported by the U.S. Department of

Energy, Office of Science, and Office of Basic Energy Sciences, under Contract DE-AC02-06CH11357. MRCAT operations are supported by the Department of Energy and the MRCAT member institutions.

References

[1] U.S.E.I. Administration, Annual Energy Review, 2010. <www.eia.gov/aer>.
[2] American Energy: The Renewable Path to Energy Security, Worldwatch Institute Center for American Progress, 2006.
[3] Energy, U.S.D.o., U.S. Billion-Ton Update: Biomass Supply for a Bioenergy and Bioproducts Industry, R.D. Perlack and B.J.S. (Leads), ORNL/TM-2011/224, Oak Ridge National Laboratory, Oak Ridge, TN, 2011, p. 227.
[4] A.S. Mamman, J.M. Lee, Y.C. Kim, I.T. Hwang, N.J. Park, Y.K. Hwang, J.S. Chang, J.S. Hwang, Biofuels, Bioprod. Bioref. 2 (2008) 438.
[5] J.P. Lange, W.D. van de Graaf, R.J. Haan, ChemSusChem 2 (2009) 437.
[6] J.C. Serrano-Ruiz, D. Wang, J.A. Dumesic, Green Chem. 12 (2010) 574.
[7] J.Q. Bond, D.M. Alonso, D. Wang, R.M. West, J.A. Dumesic, Science 327 (2010) 1110.
[8] H. Adkins, R. Connor, US Patent 2094975, The Quaker Oats Company, 1937.
[9] B.H. Wojcik, J. Ind. Eng. Chem. 40 (1948) 210.
[10] L.J. Frainier, H. Fineberg, US Patent 4302397, Ashland Oil, Inc., 1981.
[11] E.A. Preobrazhenskaya, J. Mamatov, I.P. Polyakov, US Patent 4261905, 1981.
[12] B.J. Liu, L.H. Lu, B.C. Wang, T.X. Cai, K. Iwatani, Appl. Catal. A 171 (1998) 117.
[13] P. Mastagli, US Patent 2763666, Societe Anonyme dite, 1956.
[14] S.J. Chiang, B.J. Liaw, Y.Z. Chen, Appl. Catal. A 319 (2007) 144.
[15] B.J. Liaw, S.J. Chiang, C.H. Tsai, Y.Z. Chen, Appl. Catal. A 284 (2005) 239.
[16] B.J. Liaw, S.J. Chiang, S.W. Chen, Y.Z. Chen, Appl. Catal. A 346 (2008) 179.
[17] H.X. Li, H.S. Luo, L. Zhuang, W.L. Dai, M.H. Qiao, J. Mol. Catal. A 203 (2003) 267.
[18] H.X. Li, S.Y. Zhang, H.S. Luo, Mater. Lett. 58 (2004) 2741.
[19] S.P. Lee, Y.W. Chen, Ind. Eng. Chem. Res. 38 (1999) 2548.
[20] X.F. Chen, H.X. Li, H.S. Luo, M.H. Qiao, Appl. Catal. A 233 (2002) 13.
[21] S. Swadesh, US Patent 2754304, The Quaker Oats Company, 1956.
[22] P.A. Wells, US Patent 2947707, The Quaker Oat Company, 1960.
[23] M. Bankmann, J. Ohmer, T. Tacke, US Patent 5591873, Degussa Aktiengesellschaft, 1997.
[24] R.S. Rao, R.T.K. Baker, M.A. Vannice, Catal. Lett. 60 (1999) 51.
[25] H.D. Brown, R.M. Hixon, Ind. Eng. Chem. 41 (1949) 1382.
[26] B.M. Nagaraja, A.H. Padmasri, B.D. Raju, K.S.R. Rao, J. Mol. Catal. A 265 (2007) 90.
[27] B.M. Nagaraja, V. Siva Kumar, V. Shasikala, A.H. Padmasri, B. Sreedhar, B. David Raju, K.S. Rama Rao, Catal. Commun. 4 (2003) 287.
[28] J. Kijenski, P. Winiarek, T. Paryjczak, A. Lewicki, A. Mikolajska, Appl. Catal. A 233 (2002) 171.
[29] S. Sitthisa, T. Pham, T. Prasomsri, T. Sooknoi, R.G. Mallinson, D.E. Resasco, J. Catal. 280 (2011) 17.
[30] S. Sitthisa, D. Resasco, Catal. Lett. 141 (2011) 784.
[31] W. Zhang, Y. Zhu, S. Niu, Y. Li, J. Mol. Catal. A 335 (2011) 71.
[32] S. Sitthisa, T. Sooknoi, Y. Ma, P.B. Balbuena, D.E. Resasco, J. Catal. 277 (2011) 1.
[33] H.Y. Zheng, Y.L. Zhu, B.T. Teng, Z.Q. Bai, C.H. Zhang, H.W. Xiang, Y.W. Li, J. Mol. Catal. A 246 (2006) 18.
[34] R. Rao, A. Dandekar, R.T.K. Baker, M.A. Vannice, J. Catal. 171 (1997) 406.
[35] J.T. Miller, A.J. Kropf, Y. Zha, J.R. Regalbuto, L. Delannoy, C. Louis, E. Bus, J.A. van Bokhoven, J. Catal. 240 (2006) 222.
[36] A. Limura, Y. Inoue, I. Yasumori, Bull. Chem. Soc. Jpn. 56 (1983) 2203.
[37] K.L. Deutsch, B.H. Shanks, J. Catal. 285 (2012) 235.
[38] G.R. Apai, J.R. Monnier, M.J. Hanrahan, J. Chem. Soc., Chem. Commun. (1984).
[39] C.L. Bianchi, M.G. Cattania, V. Ragaini, Surf. Interface Anal. 19 (1992) 533.
[40] F.M. Capece, V.D. Castro, C. Furlani, G. Mattogno, C. Fragale, M. Gargano, M. Rossi, J. Electron Spectrosc. Relat. Phenom. 27 (1982) 119.
[41] G. Comino, A. Gervasini, V. Ragaini, Z.R. Ismagilov, Catal. Lett. 48 (1997) 39.
[42] A. Kaddouri, N. Dupont, P. Gélin, P. Delichère, Catal. Lett. 141 (2011) 1581.
[43] M. Cinar, L.M. Castanier, A.R. Kovscek, Energy Fuels 25 (2011) 4438.
[44] S.D. Gardner, C.S.K. Singamsetty, G.L. Booth, G.-R. He, C.U. Pittman Jr., Carbon 33 (1995) 587.
[45] B. Beamson, D. Briggs (Eds.), The XPS of Polymers Database, Surface Spectra.
[46] J.R. Monnier, M.J. Hanrahan, G. Apai, J. Catal. 92 (1985) 119.
[47] A. Dandekar, M.A. Vannice, J. Catal. 178 (1998) 621.
[48] S. Mehta, G.W. Simmons, K. Klier, R.G. Herman, J. Catal. 57 (1979) 339.
[49] R.B.C. Pillai, Catal. Lett. 26 (1994) 365.
[50] F. Severino, J.L. Brito, J. Laine, J.L.G. Fierro, A.L. Agudo, J. Catal. 177 (1998) 82.
[51] E. Nishimura, Y. Inoue, I. Yasumori, Bull. Chem. Soc. Jpn. 48 (1975) 803.
[52] J.D. Stroupe, J. Am. Chem. Soc. 71 (1949) 569.
[53] C.H. Bartholomew, R.J. Farrauto, Fundamentals of Industrial Catalytic Processes, John Wiley & Sons, Inc., Hoboken, New Jersey, 2006.
[54] V. Houel, D. James, P. Millington, S. Pollington, S. Poulston, R. Rajaram, R. Torbati, J. Catal. 230 (2005) 150.
[55] A. Martínez-Arias, A.B. Hungría, G. Munuera, D. Gamarra, Appl. Catal. B 65 (2006) 207.
[56] A.A. Kozinski, US Patent 4185022, The Quaker Oats Company, 1980.
[57] J. Wu, Y. Shen, C. Liu, H. Wang, C. Geng, Z. Zhang, Catal. Commun. 6 (2005) 633.
[58] B.M. Nagaraja, V.S. Kumar, V. Shasikala, A.H. Padmasri, B. Sreedhar, B.D. Raju, K.S.R. Rao, Catal. Commun. 4 (2003) 287.
[59] B.M. Nagaraja, A.H. Padmasri, P. Seetharamulu, K.H.P. Reddy, B.D. Raju, K.S.R. Rao, J. Mol. Catal. A 278 (2007) 29.